The effects of curcumin, mangiferin, resveratrol and other natural plant products on aminopeptidase B activity

Sandrine Cadel, Cécile Darmon, Alexandre Désert, Mouna Mahbouli, Christophe Piesse, Thanos Ghélis, René Lafont, Thierry Foulon

The effects of curcumin, mangiferin, resveratrol and other natural plant products on aminopeptidase B activity

Sandrine Cadel [a,*], Cécile Darmon [a], Alexandre Désert [a], Mouna Mahbouli [a], Christophe Piesse [b], Thanos Ghélis [a], René Lafont [a], Thierry Foulon [a]

[a] Sorbonne Université, Institut de Biologie Paris Seine (IBPS), Equipe Biogenèse des Signaux Peptidiques (BIOSIPE), 75005, Paris, France
[b] Sorbonne Université, CNRS, Institut de Biologie Paris Seine (IBPS), Plate-forme Ingénierie des Protéines et Synthèse Peptidique, 75005, Paris, France

Keywords:
Aminopeptidase B
Leukotriene A_4 hydrolase
Curcumin
Mangiferin
Resveratrol

A B S T R A C T

Aminopeptidase B (Ap-B) is a Zn^{2+}-aminopeptidase of the M1 family which is implicated, in conjunction with the nardilysin endoprotease, in the generation of miniglucagon, a peptide involved in the maintenance of glucose homeostasis. Other *in vivo* physiological roles have been established for this vertebrate enzyme, such as the processing of Arg-extended forms of human insulin and cholecystokinin 9 and the degradation of viral epitopes in the cytoplasm. Among M1 family members, Ap-B is phylogenetically close to leukotriene A_4 hydrolase (LTA_4H), a bi-functional aminopeptidase also able to transform LTA_4 in LTB_4 (a lipid mediator of inflammation). As the activities of LTA_4H are reported to be inhibited by resveratrol, a polyphenolic molecule from red wine, the effect of this molecule was investigated on the Ap-B activity. Several other active phenolic compounds produced in plants were also tested. Among them, curcumin and mangiferin are the most effective inhibitors. Dixon analysis indicates that curcumin is a non-competitive inhibitor with a Ki value of 46 $\mu mol.L^{-1}$. Dixon and Lineweaver-Burk representations with mangiferin show a mixed non-competitive inhibition with Ki' and Ki values of 194 $\mu mol.L^{-1}$ and 105 $\mu mol.L^{-1}$, respectively. At 200 $\mu mol.L^{-1}$, no significant effect was observed with caffeic, chlorogenic, ferulic, salicylic and sinapic acids as well as with resveratrol. Analyses on the 3D-structure of LTA_4H with resveratrol (pdb: 3FTS) and the Ap-B 3D-model allow hypothesis to explain theses results.

1. Introduction

Aminopeptidase B (Ap-B) belongs to the M1 family of Zn^{2+}-aminopeptidases, enzymes that catalyze the hydrolysis of the peptide bond on the carbonyl side of amino acid residues present at the NH_2-terminus of peptides; the preferred target amino acid for Ap-B is a basic residue [1,2]. A further important aminopeptidase of this family is LTA_4 hydrolase (LTA_4H) which is also able to hydrolyze the epoxide function of leukotriene A_4 (LTA_4) to produce a central inflammatory lipid mediator, leukotriene B_4 (LTB_4; [3]). Ap-B is phylogenetically closely related to LTA_4H and has a residual LTA_4 hydrolase activity [4]. The enzymes of the M1 family are involved in important physiological functions in mammals. The design of specific inhibitors of these aminopeptidases is being actively investigated since they are clearly identified as major players in diverse pathologies. This is the case of Ap-A in hypertension [5], LTA_4H in inflammation [6] and Ap-N in cancers [7]. Concerning Ap-B, its catalytic properties, ubiquitous expression and various subcellular localizations allow this enzyme to mature or degrade numerous peptide substrates in mammalian cells [8]. Ap-B is implicated in the production of cholecystokinin-8, a pleiotropic neuropeptide, in the cytoplasmic degradation of an epitope of the human cytomegalovirus, in the processing of Arg-extended forms of human insulin, and in the proteolytic processing mechanism generating mini-glucagon, a peptide required to maintain glucose homeostasis [9–12]. Mini-glucagon is co-secreted with glucagon by the pancreatic α-cells and inhibits insulin secretion by β-cells [13]. Though Ap-B may also be involved in type-2 diabetes through its role in the production of mini-glucagon, it is clear that many of its physiological functions and pathological implications remain to be discovered.

Abbreviations: Ap-B, Aminopeptidase B; LTA_4H, Leukotriene A_4 hydrolase; Arg-AMC, Arg-7-amino-4-methylcoumarin; TFA, trifluoroacetic acid.

* Corresponding author. Sorbonne Université, Institut de Biologie Paris Seine (IBPS), Equipe Biogenèse des Signaux Peptidiques (BIOSIPE), 7 quai Saint Bernard, 75252, Paris cedex 05, France.
E-mail address: marie-sandrine.cadel@sorbonne-universite.fr (S. Cadel).

The phylogenetic proximity of Ap-B to LTA_4H encouraged us to test resveratrol (Table 1S, see supplementary material), a polyphenolic phytoalexin derived from red wine, on the Ap-B activity. This molecule displaying anti-aging and heart protective properties [14], is also reported to reduce the spread and growth of pancreatic cancer by inhibiting LTA_4H [15]. Moreover, different natural polyphenolic phytochemicals whose effects could impact type 2 diabetes and other pathological conditions, such as curcumin or mangiferin were also analyzed (Table 1S). Curcumin, originally isolated from the rhizome of the turmeric plant (*Curcuma longa),* has many cellular targets and plays multiple roles in protecting cells. It presents many preventative and therapeutic activities primarily against inflammation, cancer, cell oxidation, aging, Alzheimer's disease and diabetes [16–19]. Results show that curcumin inhibits Ap-B activity towards L-Arg-AMC substrate with a half-maximal inhibitory concentration (IC_{50}) similar to the Ki and equal to 46 $\mu mol\,L^{-1}$ indicating a non-competitive inhibition. Mangiferin is a xanthone, which is present in several plant species, particularly the mango *Mangifera indica*. This compound has numerous biological activities, such as a protective effect against diseases associated with oxidative stress, inflammatory response and against type 2 diabetes [20,21]. Tests with mangiferin indicate a non-competitive inhibition of Ap-B with a small mixed character. The observed K_i and K_i' values are 104 and 195 μM, respectively. These results show that, among the molecules tested, curcumin and mangiferin affect aminopeptidase B activity and open the way to search for more selective derivatives/analogues as potential inhibitors.

2. Material and methods

2.1. Chemicals

Curcumin, mangiferin, *trans*-resveratrol, chlorogenic acid and Tween-20 were supplied by Sigma-Aldrich. The sinapic and ferulic acids were supplied by Fluka. Arg-AMC (7-amino-4-methylcoumarin) and AMC were from PeptaNova. Salicylic acid comes from Alfa Aesar. Fmoc-protected amino acids were purchased from Nova Biochem. Fmoc-L-Leu-wang resin was obtained from Merck Millipore and solvents from SDS.

2.2. Synthesis and purification of peptides

Arg_0-Leu_5 and Leu_5-enkephalin were synthesized using FastMoc chemistry solid-phase procedures on an automatic peptide synthesizer (Applied Biosystems model 433A). The peptides were purified by RP-HPLC on a Phenomenex Luna C18 (10 × 250 mm, 10 μm particle size) column, eluted at a flow-rate of 5 mL/min with a linear gradient of 0–60% acetonitrile (ACN; 0.07% trifluoroacetic acid; TFA) in 0.1% TFA/H_2O (1% ACN/min). The homogeneity and identity of the synthetic peptides were evaluated by MALDI-TOF (Voyager DE-PRO, Applied Biosystems, Mass spectrometry and Proteomics Platform, IBPS, FR3631 Sorbonne Université-CNRS, Paris, France) and analytical RP-HPLC on a Phenomenex Luna C-18 (4.6 × 250 mm, 5 μM) column, using the above conditions with a flow-rate of 0.75 mL/min.

2.3. Recombinant His-tagged aminopeptidase B purification

The expression, secretion and purification of the rat recombinant His-tagged Ap-B using a baculovirus expression system was previously described in Cadel et al. [22]. Briefly, 200 mL of the recombinant baculovirus infected SF9 cells medium was concentrated and equilibrated in 20 mM Tris-HCl buffer pH 8, using a vivaflow 200 membrane (cut-off 10000 MWC; Sartorius Stedim Biotech SA). Then, the 120 mL resulting medium was adjusted to 150 mL with Tris-HCl 20 mM pH 8 and a final concentration of 0.5 M NaCl and 20 mM imidazole and applied on a 5 mL His-Trap column (GE-Healthcare). An imidazole gradient from 20 to 200 mM in Tris-HCl 20 mM pH 8 with 0.5 M NaCl was run. The eluted fractions with Ap-B activity were pooled, concentrated and equilibrated in 100 mM Tris-HCl buffer, pH 7.4, 150 mM NaCl using an Amicon membrane. The concentrated preparation was applied to an exclusion chromatography column (Hiload 16/60 Superdex 200, GE Healthcare) equilibrated with 100 mM Tris-HCl buffer, pH 7.4, 150 mM NaCl. The resulting active fractions corresponding to the monomeric protein were pooled, concentrated to 500 μL and stored at 4 °C.

2.4. Ap-B inhibition assays with different natural compounds

The assays were performed in a 100 μL reaction mixture containing 100 mM Tris-HCl buffer, pH 7.4, and 0.1% Tween 20. For determination of the kinetic parameters, a range of 0–400 μM final concentration of Arg-AMC substrate (Peptanova) and 0.5 ng of purified enzyme were used (3 independent experiments). The measurements of enzyme activity were performed on a Fluostar Galaxy spectrofluorimeter at 28 °C in which samples were excited at 380 nm and emission measured at 460 nm over 40 min. The spectrofluorimeter kinetic software allowed the calculation of the enzymatic rate ($unit.min^{-1}$) under Michaelis-Menten conditions, which was converted in $\mu mole.L^{-1}.min^{-1}$ using a standard curve established with a range of 0–1 μM AMC (mean of 3 experimental points). For determination of the inhibitory effect of natural molecules, mangiferin or curcumin were solubilized in dimethyl sulfoxide for the 10 mM concentration, or in 100 mM Tris-HCl buffer, pH 7.4, with 0.1% Tween-20 for the 1 mM and 250 μM initial concentrations. The 100 μL reaction mixture contained 20 μL of curcumin or mangiferin solubilized at concentrations varying between 0 and 1 mM, 70 μL with 1.9 ng of enzyme and 10 μL of Arg-AMC in 100 mM Tris-HCl buffer, pH 7.4, with 0.1% Tween-20. The final concentration of inhibitor varied between 0 and 200 μM and the final concentration of Arg-AMC substrate could be 10, 20, 40, 80, 100 or 120 μM.

A solution of 10 mM in ethanol was used for the other inhibitors to perform a test with 100, 200 and 400 μM final concentration in the standard Tris-HCl buffer.

To verify if curcumin could bind covalently with the enzyme, 0.8 ng enzyme was pre-incubated, or not (control), with different concentrations of curcumin (0–200 μM) during 0, 1, 2 and 4 h before addition of the substrate (20 μM final).

2.5. Kinetics analysis of Ap-B inhibition

The concentration of each compound resulting in 50% inhibition (IC_{50}) was determined by non-linear regression analysis with the Graphpad Prism software (Graphpad software). Determination of the Ki value and analysis of the inhibitory effect were obtained with the Dixon and Lineweaver-Burk representation using the Graphpad prism software. Determination of the Ki and Ki' values with the $1/V_M^{app} = f(I)$ and $K_M^{app}/V_M = f(I)$ plots was obtained with the Kaleidagraph software (Synergy software).

2.6. Ap-B assays on natural peptides

Enzymatic tests were performed using 1.3 μg purified protein, 10 μg Arg_0-Leu_5-enkephalin substrate in the absence or presence of 50 μM final concentration of curcumin, in a total volume of 100 μL containing 100 mM Tris-HCl, pH 7.4. The reaction was stopped after 1 h by addition of 0.3% (w/v) TFA. Samples were injected on to a C18

column (250 X 4,6 mm; UP5PXP-250/046; Interchim) combined with an HPLC (Waters). Peptides are eluted with a gradient of ACN (0.7% TFA) from 20 to 60% in water (0.1% TFA) at a flow-rate of 1 mL per minute for 40 min.

2.7. Molecular docking study

The resveratrol molecule was docked by superposition of the Ap-B [23] and the LTA_4H (pdb: 3FTS) structures with the DaliLite software of the Thornton group at the EMBL-EBI. Images of structures were performed using the Visual Molecular Dynamics (VMD) software (Theoretical and Computational Biophysics Group, USA). Structures of natural molecules were drawn with the MolDraw software [24].

2.8. Statistical analyses

All the tests were performed in triplicate and the standard error of the mean (SEM) was calculated.

3. Results

3.1. Determination of kinetic parameters of Ap-B with Arg-AMC substrate

Before testing the different inhibitors, the Ap-B kinetic parameters were determined with the Arg-AMC substrate. The Michaelis constant obtained (K_M) is 48 ± 2.8 μM and the maximal velocity (V_M) is 0.18 μmol L^{-1}.min^{-1} (Fig. 1S, see supplementary material). Considering that we have 70 pmoles.L^{-1} of enzyme per test, we conclude that the catalytic constant (k_{cat}) is 43 sec^{-1}.

3.2. Effect of different natural molecules on the Ap-B activity

3.2.1. Effect of resveratrol

Trans-resveratrol is reported to inhibit LTA_4H and despite the relatively high IC_{50}values, 366 μM and 212 μM for the respective peptidase and epoxide hydrolase activities, is considered as a good inhibitor of the enzyme [25]. Resveratrol with *trans*- and *cis*-configuration (Table 1S) were tested to analyze their inhibitory potential on Ap-B activity. This compound, in *trans*- or *cis*-configuration, exhibits higher IC_{50} (>400 μM) when used with Ap-B, showing an absence of significant inhibition. Resveratrol appears to be more specific to LTA_4H than to Ap-B. The analysis of the *trans*-resveratrol molecule in the 3D structure of LTA_4H (pdb: 3FTS [25]) allows us to propose a hypothesis. The hydroxyl group of the phenol from the LTA_4H Tyr^{267} residue and the hydroxyl group of resveratrol are sufficiently close to establish hydrogen bonds between them and nearby residues, such Asp^{375} (3.44 Å; Fig. 1-A; [25]). In Ap-B, similar hydrogen bonds should not be established, owing to a Phe residue in position 297 instead of a tyrosine (Fig. 1-B, [26]). Thus, *trans*-resveratrol could interact differently with the Ap-B structure, which could explain why resveratrol has no significant effect on its activity.

3.2.2. Effect of curcumin

Ap-B activity was measured in the presence of final concentrations of curcumin (Table 1S) ranging from 2.5 to 200 μmol L^{-1} in a 0.1 M Tris-HCl buffer, pH 7.4, in the presence of 0.1% Tween-20, a non-anionic detergent used to solubilize curcumin which cannot be directly dissolved in water. This percentage does not inhibit Ap-B activity. IC_{50} values were determined using 4 different concentrations of the Arg-AMC substrate: 20, 40, 80 and 120 μmol L^{-1} (Fig. 2S, see supplementary material). Results show that the IC_{50} values are relatively close with an average of approximately 46 μmol L^{-1}, regardless of substrate concentration, indicating that curcumin is a non-competitive inhibitor. The Dixon linear representation (Fig. 2) confirmed this hypothesis because the three straight lines cut the X-axis at the same point. This intersection point corresponds to the K_i and gives a value of 46 μmol L^{-1}, similar to the IC_{50}, confirming non-competitive inhibitor behaviour. No significant difference of activity was observed when the enzyme was preincubated with curcumin during 10 min, 1, 2 and 4 h before addition of the substrate, suggesting that the inhibition of Ap-B is not irreversible at least during this period (data not shown).

An Ap-B physiological peptide substrate was used to confirm the curcumin inhibitory effect observed with the Arg-AMC chromogenic substrate. The assays were achieved with or without 50 μM curcumin, and with an Arg_0-Leu_5-enkephalin substrate (Arg-Tyr-Gly-Gly-Phe-Leu). The HPLC elution profiles of the substrate (peak 1: Arg-Tyr-Gly-Gly-Phe-Leu) and the product (peak 2: Tyr-Gly-Gly-Phe-Leu) show that curcumin inhibits the Ap-B activity at a concentration of 50 μM (Fig. 3S, see supplementary material). A mass spectrometry analysis confirmed the identity of each peptide contained in these peaks, the Arg_0-Leu_5-enkephalin substrate in peak 1 with a monoisotopic mass of 712.35 g mol^{-1} and the Leu_5-

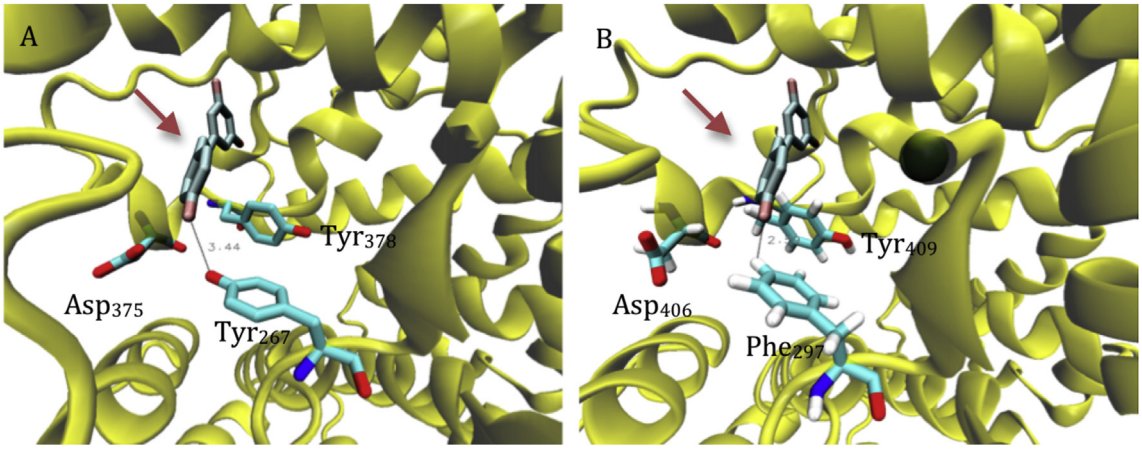

Fig. 1. (A) Schematic representation showing resveratrol, indicated with an arrow, in a pocket of the 3D structure of the LTA_4H enzyme (pdb: 3FTS). A hydrogen interaction between Tyr^{267} and the hydroxyl group of the phenol radical of resveratrol is shown (3.44 Å distance; [25]). (B) The resveratrol molecule was docked by superposition of the 3D Ap-B model and the LTA_4H structure with the DaliLite software (Thornton group, EMBL-EBI). Images of structures were performed using the Visual Molecular Dynamics (VMD) software.

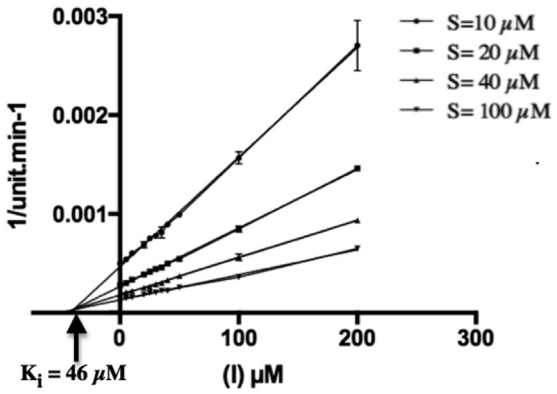

Fig. 2. Effect of curcumin on Ap-B activity. Dixon representation, 1/v (min.-slope^{-1}) = f(curcumin; I), with 4 different concentrations of Arg-AMC substrate that allows to determine the K_i value (46 μM).

enkephalin product in peak 2 with a monoisotopic mass of 556.26 g mol^{-1} (Fig. 4S, see supplementary material).

Taking into consideration the similarity between curcumin and resveratrol owing to their polyphenolic character, it is possible that curcumin enters the Ap-B structure in the same pocket as resveratrol in the LTA_4H. The superposition of two different 3D structures of LTA_4H (root mean square deviation of 0.2 Å), one containing the tripeptide Arg-Ala-Arg (RAR) substrate in the active site (pdb: 3B7T) and one containing resveratrol (pdb: 3FTS), allows verifying that the inhibitor does not occupy the same site as the substrate (Fig. 3). Moreover, the inhibition mechanism seems also to be a non-competitive process, since crystal structure of LTA_4H was obtained in presence of dihydroresveratrol and bestatin (pdb: 3FTX), a competitive inhibitor.

3.2.3. *Effect of mangiferin*

Tests with mangiferin (Table 1S) were achieved similarly as for curcumin. Results suggest that mangiferin is mainly a non-competitive inhibitor with a slightly mixed behaviour. Indeed, the Dixon representation shows that the straight lines cross slightly above the X-axis (Fig. 5S–A, see supplementary material). It is also the case for the Lineweaver-Burk representation, confirming the non-competitive and mixed inhibitory properties of mangiferin (Fig. 5S–B). The subsequent graphs $1/V_M^{app} = f(I)$ and $K_M^{app}/V_M = f(I)$ allow the determination of the respective K_i' (194 μM) and K_i (105 μM) values (Fig. 5S–C-5S-D).

3.2.4. *Other tested molecules*

Among the other molecules tested, ferulic acid, which corresponds to a truncated form of curcumin, and other acids like chlorogenic, salicylic, caffeic and sinapic acids (Table 1S) did not inhibit Ap-B activity at 200 μM (data not shown). A possible hypothesis is that the carboxylic group of these molecules with its negative charge hampers the binding. This has to be considered since the recognition of the Arg-AMC substrate implies ionic interactions between the guanidinium group of the arginine of the substrate and the Asp^{406} located near the binding site of the

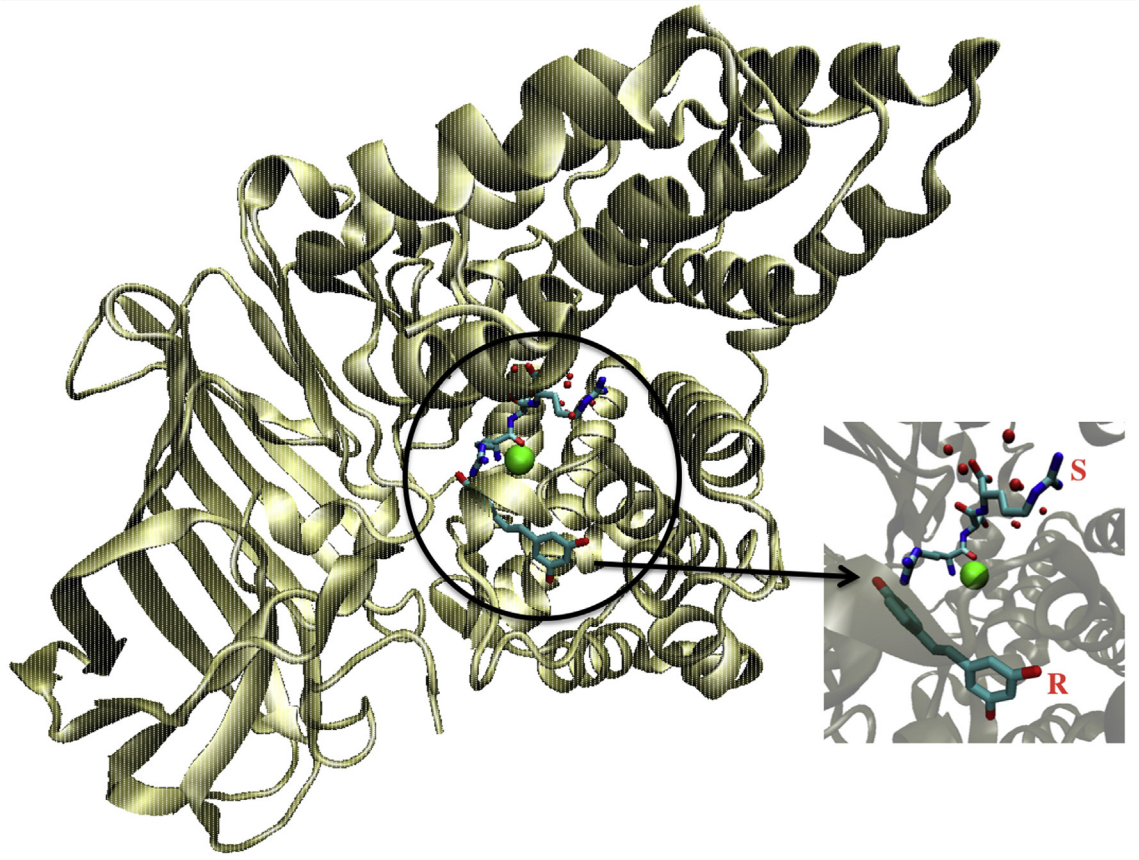

Fig. 3. Superposition of the 3B7T and 3FTS structures of the LTA_4 hydrolase using DaliLite software. The tripeptide substrate RAR (S) and the resveratrol (R) are indicated. The zinc atom is symbolized by a green sphere and small red spheres represent water molecules.

inhibitor (Fig. 1; [27]).

4. Discussion

One of our goals was to test different natural molecules from plants on Ap-B activity. Among the molecules isolated from plants with potential benefits on human health and a significative effect on Ap-B activity, there is curcumin. This phenolic compound interacts with several cellular targets including transcription factors, enzymes, cellular cycle proteins, cytokines and receptors, with either activator or inhibitor effects on expression and/or activity [28]. This infers potential activity in many biological responses like anti-inflammatory, anti-cancerous or anti-diabetic activity [16–19]. Curcumin is a non-competitive inhibitor of phosphorylase kinase with a K_i of 75 μM [29] and of aminopeptidase N with a K_i of 11.2 μM [30]. In the case of Ap-N, the inhibition is irreversible and allow inhibition of tumour angiogenesis [30]. Our results show that curcumin inhibits Ap-B in a non-competitive way with a K_i of 46 μM with the Arg-AMC substrate. No irreversible character has been observed. This inhibitory effect is also observed at 50 μM when a physiological peptide substrate, Arg_0-Leu_5-enkephalin, is used. Curcumin appears to be a modest inhibitor of Ap-B, but nevertheless useable if one refers to the amounts used in therapeutic assays [31]. Moreover, since it is a non-competitive inhibitor, its effect on Ap-B activity is independent of substrate concentration. Curcumin has multiple effects and acts on many targets according to different mechanisms in many physiological and pathophysiological processes [32]. This constitutes a major difficulty in understanding its modes of action. As in the case of phosphorylase kinase, where direct inhibition of the enzyme results in significant physiological effects by influencing some signaling pathways [33], inhibition of Ap-B by curcumin can block the biosynthesis of peptides, thereby causing a cascade of events that amplify the physiological response of the cells or organisms.

Concerning mangiferin and when compared to curcumin, Ap-B has a lower affinity (around 2.3–4.3-fold less; $K_i = 105$ μM and $K_i' = 195$ μM). The structure of mangiferin is derived from xanthone with phenol and glucose groups leading to a more hydrophilic and bulkier molecule than curcumin (Table 1S). Binding of mangiferin to Ap-B acts as a mixed non-competitive inhibitor mechanism. As the K_i is inferior to K_i' (105 versus 195 μM), increasing the inhibitor concentration decreases the affinity of the enzyme towards its substrate.

The confirmation of the inhibitory effect of molecules such as curcumin or mangiferin on Ap-B activity must now be demonstrated in biological systems to identify the importance of the physiological role of Ap-B. For example, the design of more potent inhibitors and their comparison with curcumin analogues, characterized for their hypoglycemic properties [34], could make it possible to specify the role of Ap-B in pathologies such as type 2 diabetes. Indeed, this enzyme, secreted by the α cells of pancreas, is implicated in the production of miniglucagon [12], a potent inhibitor (pM range) of insulin secretion in islets of Langerhans. So, Ap-B could be a target in case of impaired insulin secretion owing to an excess of miniglucagon [13]. Then it would be interesting to study in detail the effect of these inhibitors on the production of miniglugagon in these cells, as well as its possible consequences on the expression and secretion of Ap-B in order to identify potential indirect effects. One of the main difficulties of this type of study is that Ap-B is a processing enzyme which intervenes after a first specific cleavage by an endoprotease, such the NRD convertase (or nardilysin) in the case of miniglucagon [1,8,12] or the cathepsin L in the case of cholecystokinin-8 [9]. It is therefore necessary to study in parallel the effects of both natural molecules on the different endoproteases in order to determine the consequences of the inhibition of the Ap-B in a physiological process. Moreover, they may be direct or indirect, as in the case of prohormone convertases, where a loss of their activities is mediated by a limitation of the Ca^{2+} import into the endoplasmic reticulum [35].

Author contribution

SC, TF and RL conceived and designed the experiments. SC, CD, AD, MM and TG performed the experiments. CP synthetizes the peptide substrates. SC and AD analyzed and interpreted the data. SC and AD performed the computation work. SC and TF wrote the paper prepared figures and/or table. SC, RL, TF and TG rewiewed drafts of the paper.

Acknowledgements

We would like to thanks G. Bolbach and G. Clodic (Laboratoire des Biomolécules, UMR 7203 Sorbonne Université-CNRS, Paris, France) for their help and technical expertise, Michèle Reboud for her advices during the preparation of the manuscript and Guy Hervé and Laurence Dinan for their advices and the careful reading of the manuscript.

Appendix A. Supplementary data

Supplementary data to this article can be found online at https://doi.org/10.1016/j.bbrc.2019.02.143.

Transparency document

Transparency document related to this article can be found online at https://doi.org/10.1016/j.bbrc.2019.02.143.

Funding

This work was supported by funds from the Sorbonne Université - Faculté des sciences et d'ingénierie and the Centre National de la Recherche Scientifique (CNRS).

References

[1] S. Cadel, A.R. Pierotti, T. Foulon, et al., Aminopeptidase-B in the rat testes: isolation, functional properties and cellular localization in the seminiferous tubules, Mol. Cell. Endocrinol. 110 (1995) 149–160. http://www.ncbi.nlm.nih.gov/pubmed/7672445.

[2] T. Foulon, S. Cadel, A. Prat, et al., NRD convertase and aminopeptidase B: two processing metallopeptidases with a selectivity for basic residues, Ann. Endocrinol. 58 (1997) 357–364. http://www.ncbi.nlm.nih.gov/pubmed/9685993.

[3] O. Rådmark, T. Shimizu, H. Jörnvall, B. Samuelsson, Leukotriene A4 hydrolase in human leukocytes. Purification and properties, J. Biol. Chem. 259 (1984) 12339–12345. http://www.ncbi.nlm.nih.gov/pubmed/6490615.

[4] S. Cadel, T. Foulon, A. Viron, et al., Aminopeptidase B from the rat testis is a bifunctional enzyme structurally related to leukotriene-A4 hydrolase, Proc. Natl. Acad. Sci. U.S.A. 94 (1997) 2963–2968. http://www.ncbi.nlm.nih.gov/pubmed/9096329.

[5] Y. Yang, C. Liu, Y.-L. Lin, F. Li, Structural insights into central hypertension regulation by human aminopeptidase A, J. Biol. Chem. 288 (2013) 25638–25645, https://doi.org/10.1074/jbc.M113.494955.

[6] A. Rinaldo-Matthis, J.Z. Haeggström, Structures and mechanisms of enzymes in the leukotriene cascade, Biochimie 92 (2010) 676–681, https://doi.org/10.1016/j.biochi.2010.01.010.

[7] B. Sanz, I. Perez, M. Beitia, et al., Aminopeptidase N activity predicts 5-year survival in colorectal cancer patients, J. Investig. Med. 63 (2015) 740–746, https://doi.org/10.1097/JIM.0000000000000199.

[8] S. Cadel, C. Piesse, V.L. Pham, et al., Aminopeptidase B, in: A.J. Barrett, N.D. Rawlings, J.F. Woesner (Eds.), Handbook of Proteolytic Enzymes, third ed., Academic Press, London, 2011, pp. 473–479.

[9] M.C. Beinfeld, L. Funkelstein, T. Foulon, et al., Cathepsin L plays a major role in cholecystokinin production in mouse brain cortex and in pituitary AtT-20 cells: protease gene knockout and inhibitor studies, Peptides 30 (2009) 1882–1891, https://doi.org/10.1016/j.peptides.2009.06.030.

[10] S. Urban, K. Textoris-Taube, B. Reimann, et al., The efficiency of human cytomegalovirus pp65495-503 CD8+ T cell epitope generation is determined by the balanced activities of cytosolic and endoplasmic reticulum-resident peptidases, J. Immunol. 189 (2012) 529–538, https://doi.org/10.4049/jimmunol.1101886.
[11] M. Kouach, B. Desbuquois, F. Authier, Endosomal proteolysis of internalised [ArgA0]-human insulin at neutral pH generates the mature insulin peptide in rat liver in vivo, Diabetologia 52 (2009) 2621–2632, https://doi.org/10.1007/s00125-009-1551-0.
[12] G. Fontés, A.-D. Lajoix, F. Bergeron, et al., Miniglucagon (MG)-Generating endopeptidase, which processes glucagon into MG, is composed of N-arginine dibasic convertase and aminopeptidase B, Endocrinology 146 (2005) 702–712, https://doi.org/10.1210/en.2004-0853.
[13] S. Dalle, G. Fontés, A.-D. Lajoix, et al., Miniglucagon (glucagon 19-29): a novel regulator of the pancreatic islet physiology, Diabetes 51 (2002) 406–412. http://www.ncbi.nlm.nih.gov/pubmed/11812748.
[14] J.A. Baur, D.A. Sinclair, Therapeutic potential of resveratrol: the in vivo evidence, Nat. Rev. Drug Discov. 5 (2006) 493–506, https://doi.org/10.1038/nrd2060.
[15] N. Oi, C.-H. Jeong, J. Nadas, et al., Resveratrol, a red wine polyphenol, suppresses pancreatic cancer by inhibiting leukotriene A4 hydrolase, Cancer Res. 70 (2010) 9755–9764, https://doi.org/10.1158/0008-5472.CAN-10-2858.
[16] M. Heger, R.F. van Golen, M. Broekgaarden, M.C. Michel, The molecular basis for the pharmacokinetics and pharmacodynamics of curcumin and its metabolites in relation to cancer, Pharmacol. Rev. 66 (2013) 222–307, https://doi.org/10.1124/pr.110.004044.
[17] S. Ghosh, S. Banerjee, P.C. Sil, The beneficial role of curcumin on inflammation, diabetes and neurodegenerative disease: a recent update, Food Chem. Toxicol. 83 (2015) 111–124, https://doi.org/10.1016/j.fct.2015.05.022.
[18] P. Potter, Curcumin: a natural substance with potential efficacy in Alzheimer's disease, J. Exp. Pharmacol. 5 (2013) 23, https://doi.org/10.2147/JEP.S26803.
[19] L.-R. Shen, L.D. Parnell, J.M. Ordovas, C.-Q. Lai, Curcumin and aging, Biofactors 39 (2013) 133–140, https://doi.org/10.1002/biof.1086.
[20] A.J.N. Sellés, D.G. Villa, L. Rastrelli, Mango polyphenols and its protective effects on diseases associated to oxidative stress, Curr. Pharmaceut. Biotechnol. 16 (2015) 272–280. http://www.ncbi.nlm.nih.gov/pubmed/25658517.
[21] T. Miura, H. Ichiki, I. Hashimoto, et al., Antidiabetic activity of a xanthone compound, mangiferin, Phytomedicine 8 (2001) 85–87. http://www.ncbi.nlm.nih.gov/pubmed/11315760.
[22] S. Cadel, C. Gouzy-Darmon, S. Petres, et al., Expression and purification of rat recombinant aminopeptidase B secreted from baculovirus-infected insect cells, Protein Expr. Purif 36 (2004) 19–30, https://doi.org/10.1016/j.pep.2004.03.013.
[23] V.-L. Pham, M.-S. Cadel, C. Gouzy-Darmon, et al., Aminopeptidase B, a glucagon-processing enzyme: site directed mutagenesis of the Zn2+-binding motif and molecular modelling, BMC Biochem. 8 (2007) 21, https://doi.org/10.1186/1471-2091-8-21.
[24] J.-M. Cense, MolDraw: molecular graphics for the macintosh, Tetrahedron Comput. Methodol. 2 (1989) 65–71, https://doi.org/10.1016/0898-5529(89)90030-4.
[25] D.R. Davies, B. Mamat, O.T. Magnusson, et al., Discovery of leukotriene A4 hydrolase inhibitors using metabolomics biased fragment crystallography, J. Med. Chem. 52 (2009) 4694–4715, https://doi.org/10.1021/jm900259h.
[26] S. Cadel, C. Darmon, J. Pernier, et al., The M1 family of vertebrate aminopeptidases: role of evolutionarily conserved tyrosines in the enzymatic mechanism of aminopeptidase B, Biochimie 109 (2015) 67–77, https://doi.org/10.1016/j.biochi.2014.12.009.
[27] K.M. Fukasawa, J. Hirose, T. Hata, Y. Ono, Aspartic acid 405 contributes to the substrate specificity of aminopeptidase B, Biochemistry 45 (2006) 11425–11431, https://doi.org/10.1021/bi0604577.
[28] H. Zhou, C.S. Beevers, S. Huang, The targets of curcumin, Curr. Drug Targets 12 (2011) 332–347. http://www.ncbi.nlm.nih.gov/pubmed/20955148.
[29] S. Reddy, B.B. Aggarwal, Curcumin is a non-competitive and selective inhibitor of phosphorylase kinase, FEBS Lett. 341 (1994) 19–22. http://www.ncbi.nlm.nih.gov/pubmed/7511111. (Accessed 21 November 2018).
[30] J.S. Shim, J.H. Kim, H.Y. Cho, et al., Irreversible inhibition of CD13/aminopeptidase N by the antiangiogenic agent curcumin, Chem. Biol. 10 (2003) 695–704. http://www.ncbi.nlm.nih.gov/pubmed/12954328.
[31] C.-H. Hsu, A.-L. Cheng, Clinical studies with curcumin, in: Mol. Targets Ther. Uses Curcumin Heal. Dis, Springer US, Boston, MA, 2007, pp. 471–480, https://doi.org/10.1007/978-0-387-46401-5_21.
[32] A.B. Kunnumakkara, D. Bordoloi, G. Padmavathi, et al., Curcumin, the golden nutraceutical: multitargeting for multiple chronic diseases, Br. J. Pharmacol. 174 (2017) 1325–1348, https://doi.org/10.1111/bph.13621.
[33] M.C.Y. Heng, Signaling pathways targeted by curcumin in acute and chronic injury: burns and photo-damaged skin, Int. J. Dermatol. 52 (2013) 531–543, https://doi.org/10.1111/j.1365-4632.2012.05703.x.
[34] K.K. Das, N. Razzaghi-Asl, S.N. Tikare, et al., Hypoglycemic activity of curcumin synthetic analogues in alloxan-induced diabetic rats, J. Enzym. Inhib. Med. Chem. 31 (2016) 99–105, https://doi.org/10.3109/14756366.2015.1004061.
[35] J. Zhu, G. Bultynck, T. Luyten, et al., Curcumin affects proprotein convertase activity: elucidation of the molecular and subcellular mechanism, Biochim. Biophys. Acta Mol. Cell Res. 1833 (2013) 1924–1935, https://doi.org/10.1016/J.BBAMCR.2013.04.002.

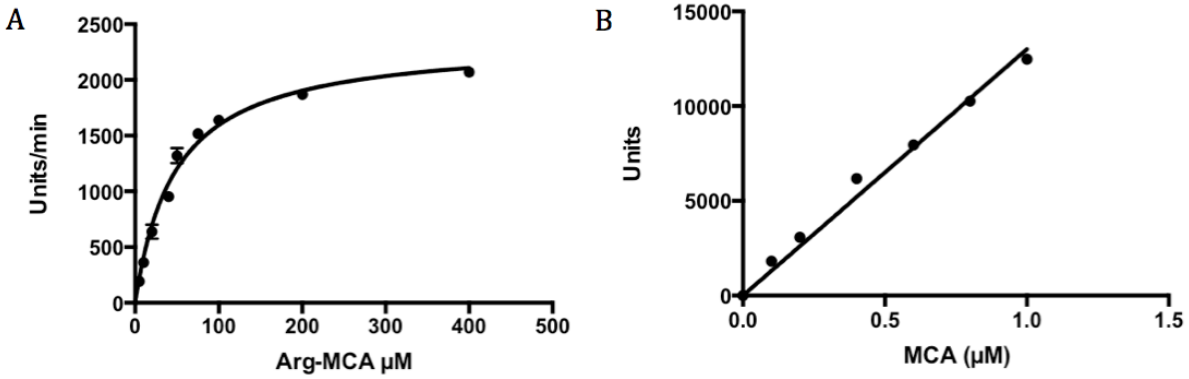

Figure 1S: Determination of Ap-B kinetic parameters with Arg-MCA substrate. (A) Michaelis curve: v (slope.min^{-1}) = f (Arg-MCA in μmole.L^{-1}). The maximal velocity (V_M) is 2361 U/min^{-1}. (B) Standard curve showing the correspondence between the concentration of MCA product (μmol.L^{-1}) and the fluorescence units (y = 13004 x).

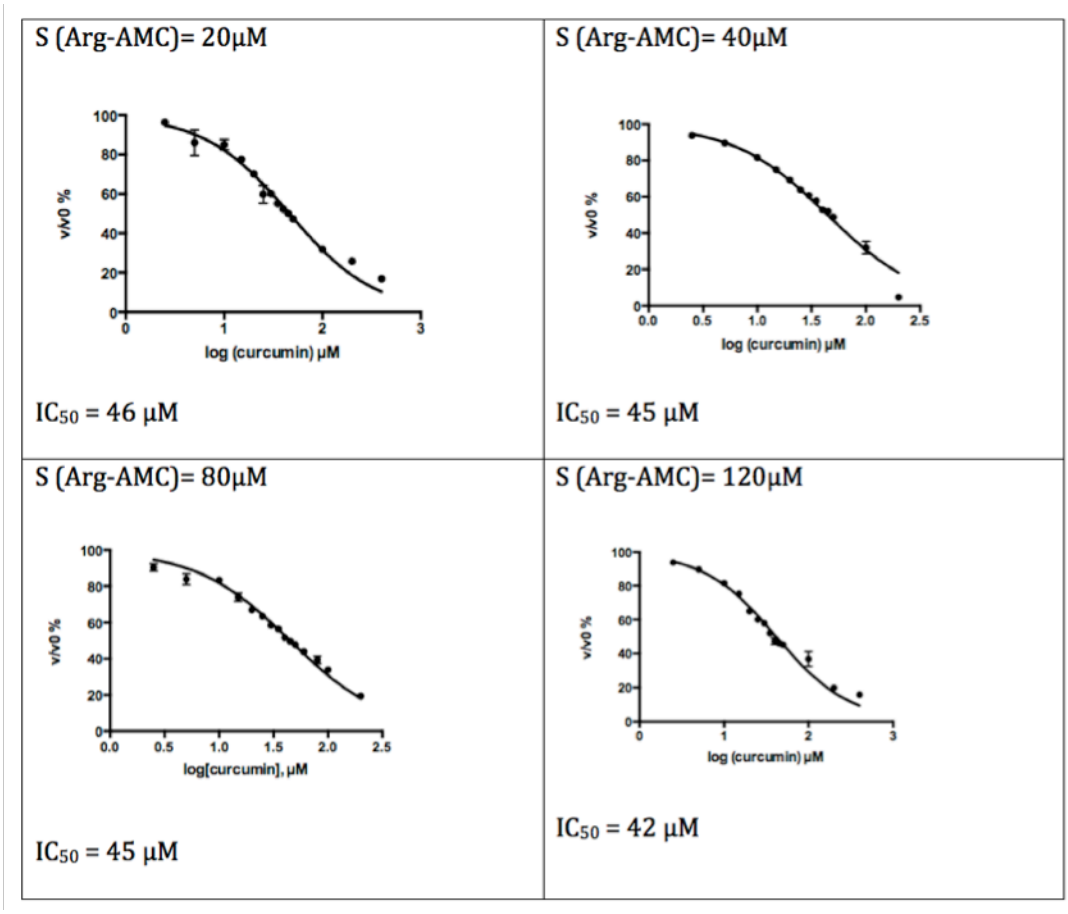

Figure 2S. Curves representing the ratio in percentages of the velocity in the presence of the curcumin inhibitor relative to the rate without inhibitor as a function of the log of concentration of inhibitor in µmol.L^{-1}. Four different concentrations of Arg-AMC substrate were used. This curve is used to determine the concentration of inhibitor giving 50% inhibition (IC_{50}).

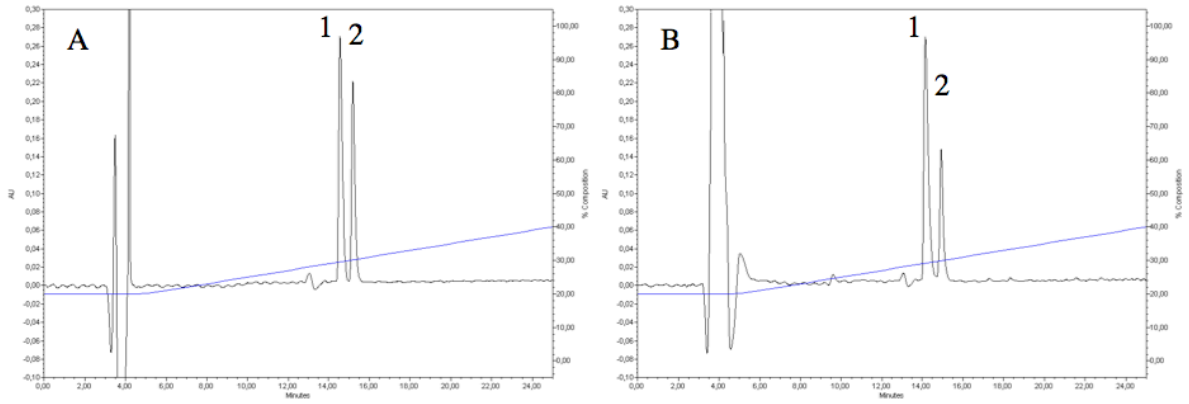

Figure 3S. HPLC profile showing the enzymatic activity of the Ap-B with the Arg_0-Leu_5enkephalin substrate (A). The acetonitrile gradient (blue line) is indicated in percentage. Peak 1 corresponds to the Arg_0-Leu_5-enkephalin substrate and peak 2 to the Leu_5-enkephalin hydrolysis product. (B) HPLC profile showing the enzymatic activity of Ap-B with the Arg_0-Leu_5-enkephalin substrate in presence of 50 μmol. L^{-1} of curcumin.

Supplementary material

Peak 1 : RYGGFL

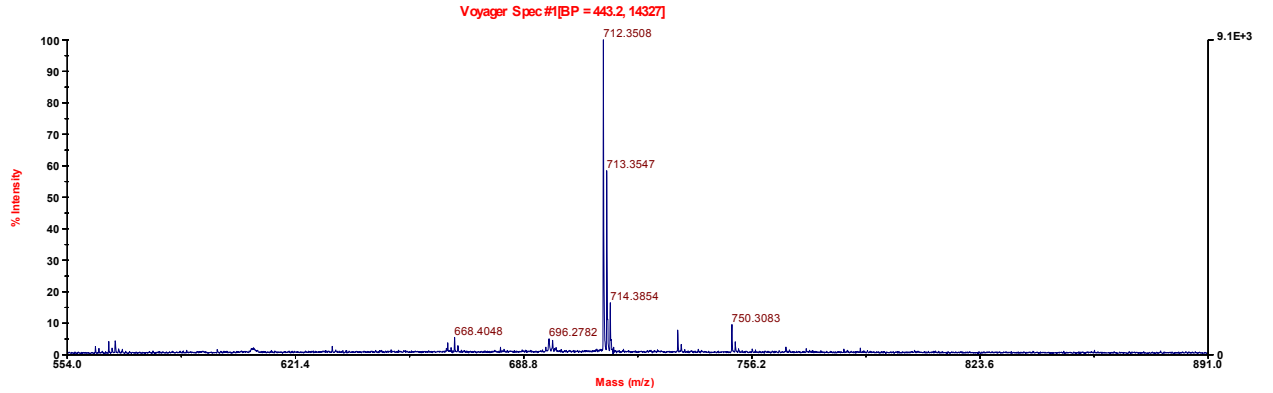

Peak 2 : YGGFL

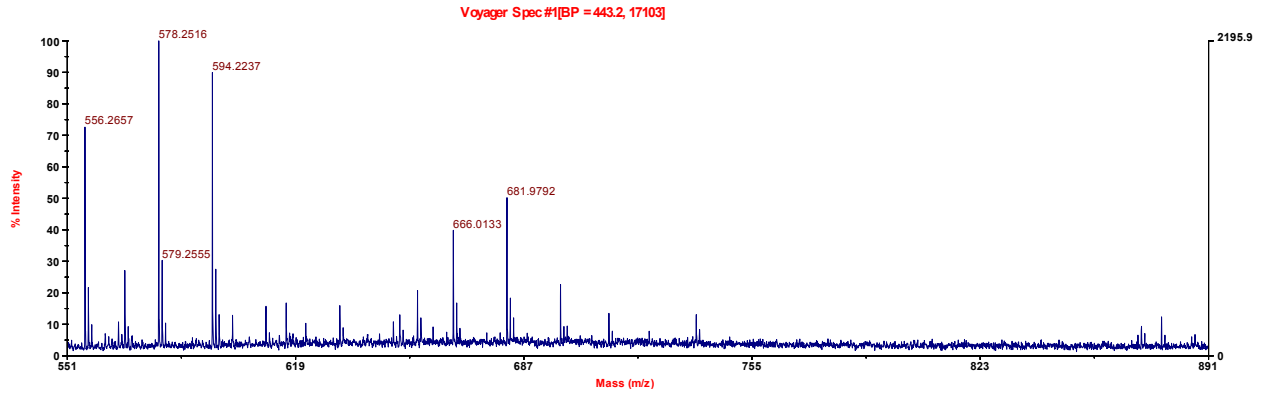

Figure 4S. Mass spectrometry analysis of Peaks 1 and 2 (MALDI-TOF). The presence of the peptide RYGGFL is confirmed in Peak 1 by the signal with a monoisotopic mass of 712.3508 Da. The presence of the peptide YGGFL is confirmed in Peak 2 by the signal with monoisotopic mass of 556.2657 Da.

Mass Spectrometry Analysis

Following HPLC fractionation, peaks 1 and 2, corresponding respectively to the Arg_0-Leu_5-enkephalin peptide substrate and to the Leu_5-enkephalin hydrolysis product were recovered. The eluates were dried, taken up in 10 μL of 0.1% trifluoroacetic acid (TFA), and diluted 10-fold in 0.1% TFA. Samples contained about 35 and 45 pmol of each peptide, respectively. For each peptide, a 1:1 mixture with the α-cyano-4-hydroxycinnamic acid (HCCA) matrix was prepared and deposited on a MALDI plate. Analysis by MALDI-TOF mass spectrometry (Voyager DE-Pro, Applied Biosystem) allowed efficient detection of each of the peptides. The presence of Arg_0-Leu_5 enkephalin peptide was confirmed in Peak 1 with the peak having a monoisotopic mass of 712.3508. Similarly, the presence of the peptide Arg_0-Leu_5 enkephalin was confirmed in the fraction of Peak 2 by detecting the monoisotopic mass peak 556.2657.

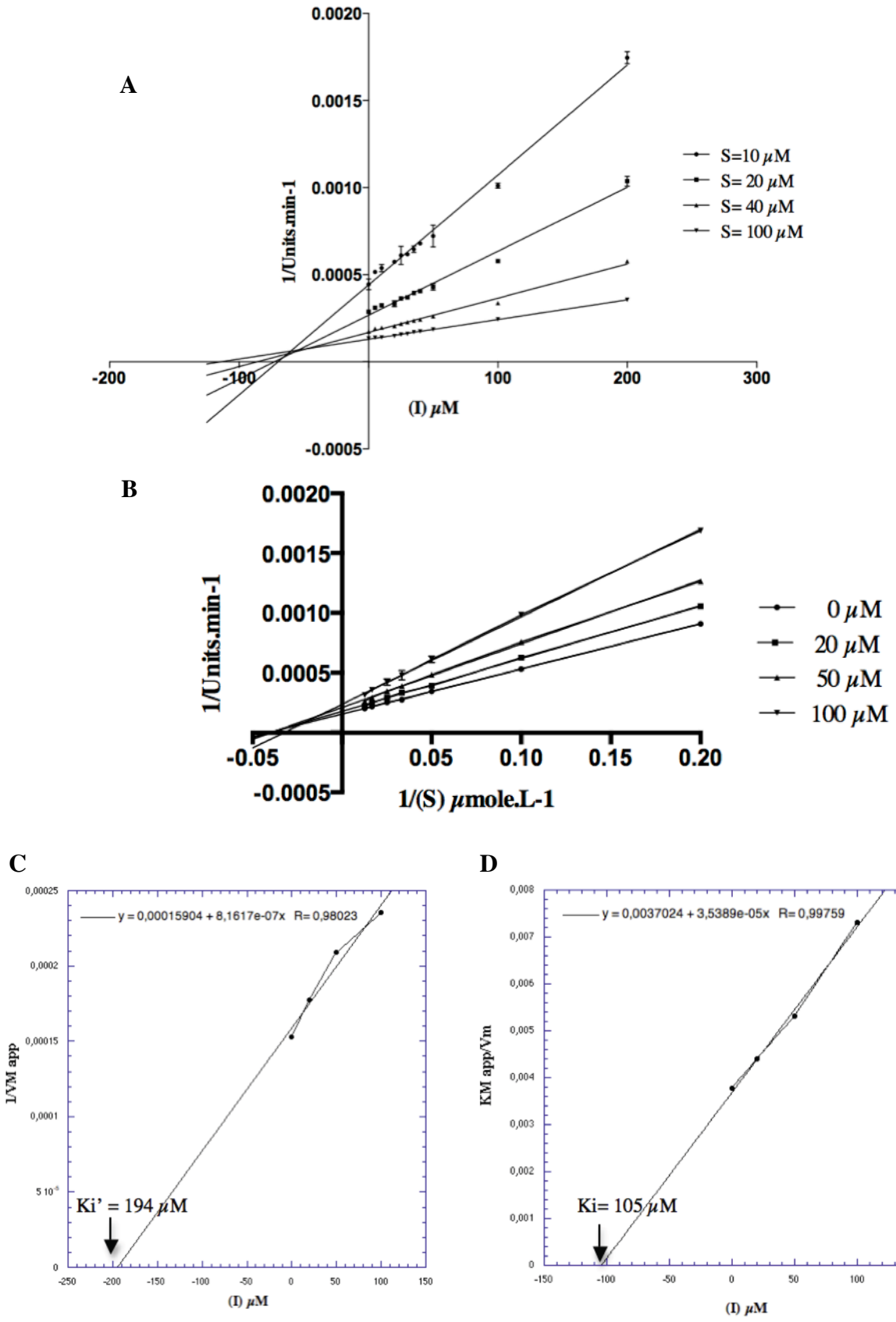

Figure 5S. Effect of mangiferin on Ap-B activity. (A) Dixon representation, 1/v = f(mangiferin; I), with 4 different concentrations of Arg-AMC substrate. (B) Lineweaver-Burk representation, 1/v = f(1/S), with the Arg-AMC substrate and 4 different concentrations of mangiferin. The graphs (C), $1/V_M^{app}$ = f(I), and (D), K_M^{app}/V_M = f(I), allow the determination of the indicated Ki' and Ki values of mangiferin using Arg-AMC substrate.

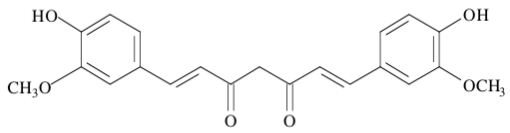 **Curcumin** **(*E*,*E*)-1,7-bis(4-Hydroxy-3-methoxyphenyl)-1,6-heptadiene-3,5-dione**	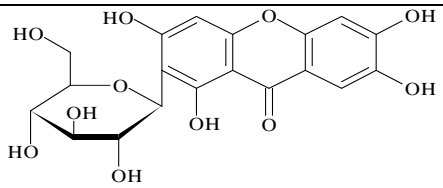 **Mangiferin** **1,3,6,7-Tetrahydroxyxanthone C_2-β -D-glucoside**
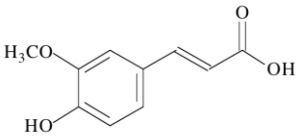 **Ferulic acid** ***trans*-4-Hydroxy-3-methoxycinnamic acid**	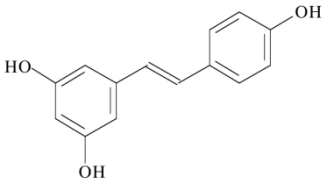 ***Trans*-resveratrol** **3,4′,5-Trihydroxy-*trans*-stilbene, 5-[(1*E*)-2-(4-Hydroxyphenyl)ethenyl]-1,3-benzenediol**
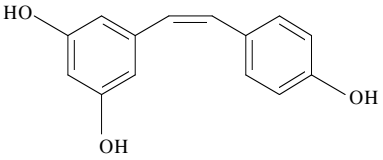 ***Cis*-resveratrol** **3,4′,5-Trihydroxy-*cis*-stilbene, 5-[(1*E*)-2-(4-Hydroxyphenyl)ethenyl]-1,3-benzenediol**	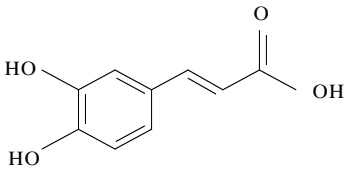 **Caffeic acid** **3,4-Dihydroxybenzeneacrylic acid, 3,4-Dihydroxycinnamic acid, 3-(3,4-Dihydroxyphenyl)-2-propenoic acid**
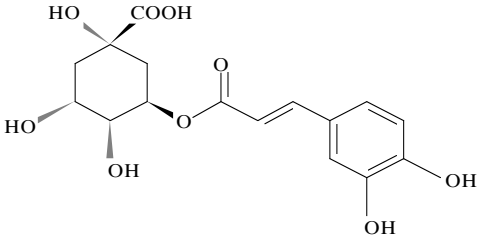 **Chlorogenic acid** **1,3,4,5-Tetrahydroxycyclohexanecarboxylic acid 3-(3,4-dihydroxycinnamate), 3-(3,4-Dihydroxycinnamoyl)quinic acid**	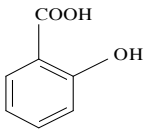 **Salicylic acid** **2-Hydroxybenzoic acid**

Table 1S: Structure of natural molecules used in the present study. Trivial and systematic names of these molecules are included.